Amino Ethyl-Functionalized SBA-15: A Promising Adsorbent for Anionic and Cationic Dyes Removal

Hajiaghababaei, Leila*+; Abozari, Saeede

Department of Chemistry, Yadegar -e- Imam Khomeini (RAH) Shahre Rey Branch, Islamic Azad University, Tehran, I.R. IRAN

Badiei, Alireza; Zarabadi Poor, Pezhman

School of Chemistry, University College of Science, University of Tehran, Tehran, I.R. IRAN

Dehghan Abkenar, Shiva

Department of Chemistry, Savadkooh Branch, Islamic Azad University, Mazandaran, I.R. IRAN

Ganjali, Mohammad Reza

Center of Excellence in Electrochemistry, Faculty of Chemistry, University of Tehran, Tehran, I.R. IRAN

Mohammadi Ziarani, Ghodsi

Department of Chemistry, Alzahra University, Tehran, I.R. IRAN

ABSTRACT: *Batch Adsorption of Acid Red 37 (AR37) and Basic Orange 2 (BO2) on amino ethyl-functionalized SBA-15 have been studied. SBA-15 was synthesized and functionalized according to the procedure in the literature. Amino ethyl-functionalized SBA-15 showed the BET surface area 520 m^2/g and pore diameter 7.02 nm, based on adsorption-desorption of N_2. SEM image shows lengthy fiber-like morphology for the title material. The presence of organic groups in the silica framework was demonstrated by thermogravimetric analysis. The effects of pH, contact time and dye concentration on adsorption were investigated in order to find the optimum adsorption conditions. The results have indicated that modification of adsorbent with a functional group of amino ethyl will remarkably increase the elimination of these two dyes but amino ethyl-functionalized SBA-15 has higher affinity to AR37. The experimental data were analyzed using the Langmuir and Freundlich adsorption models. The data fitted well to the Langmuir model with maximum adsorption capacities 333.3 for Acid Red 37 and 250.0 for Basic Orange 2. Finally, this methodology was applied for the removal of the pollutant dyes from textile wastewater. The results were shown that amino ethyl-functionalized nanoporous SBA-15 acts as an effective sorbent for the removal of both anionic and cationic dyes from aqueous solution.*

KEYWORDS: *Dye removal; Acid Red 37; Basic Orange 2; Amino ethyl-functionalized SBA-15.*

* *To whom correspondence should be addressed.*
+ E-mail: lhajiaghababaei@yahoo.com , lhajiaghababaei@iausr.ac.ir
1021-9986/2017/1/97 12/$/6.10

INTRODUCTION

Dyes are an important class of the pollution which applied in many industries, such as textile, paper, printing, food, cosmetics, etc [1]. Most industrial dyes have undesirable properties such as toxicity and mutagenesis [2] and unfortunately, most of them are stable and resistant to photodegradation, biodegradation and oxidizing agents [3]. Water pollution which comes from industrial wastewater has become a common problem for many countries [4-6]. Removal of dyes from water is very important because the water quality is greatly affected by the color of dyes. The presence of very small concentrations of dyes (less than 1 mg/L) in water is highly visible and is considered unpleasant. Besides that, many of these dyes also cause health problems such as allergic dermatitis, skin irritation, cancer and mutation in human [7-9].

A wide range of methods including adsorption [10-15], chemical oxidation [16], electrochemical oxidation [17, 18], and photocatalytic oxidation [19] are used to treat dye-laden wastewaters. Physical adsorption has been shown to be an effective method for the dye removal from the process or waste effluents. Activated carbon is a dominant and widely used adsorbent in the liquid-phase adsorption, especially in wastewater treatment. However, activated carbon suffers from slow adsorption kinetics and low adsorption capacity of bulky molecules due to the microporous structure of activated carbon. After the blockage of micropores, diffusing of macromolecules into the pores becomes difficult and inhibits the performance of bulky molecules adsorption on activated carbon [20-22]. The ideal adsorbent should have a stable and accessible pore structure with uniform pore size distribution as well as the high surface area. Ordered nanoporous silica such as MCM-41[23], LUS-1 [24, 25], and SBA-15 [26] and mesoporous carbons [27-29] with very high surface area, uniform open form structure and extremely narrow pore size distribution has great potential for application in many fields such as catalysts [30], preconcentration of metals [31-33], drug delivery [34], and modified carbon paste electrodes [35] and dyes removal [36-39]. In 1998, *Zhao et al.* [40] synthesized a new type of nanoporous material called SBA, with uniform hexagonal structure. SBA-15 is among the most popular mesoporous silicas because it has many attractive characteristics such as large surface area, high porosity, controllable and narrowly distributed pore sizes, and an ordered pore arrangement. In addition, SBA-15 has some of the largest mesopores (5–30 nm), which allow unhindered accessibility of the internal surface of the material, leading to fast kinetics of chemical or physical processes[41,42]. For adsorption processes, a variety of functional groups can be grafted or incorporated on the surface of mesoporous channels and prepare highly effective adsorbents [35, 43].

In the present study, amino ethyl-functionalized SBA-15 (AEF-SBA-15) was applied to the removal of Acid Red 37 (AR37) (Fig. 1.a) and Basic Orange 2 (BO2) (Fig. 1.b) and the dye sorption capacities of adsorbent were compared in a single dye solution. The functionalized SBA-15 was prepared and characterized. The applicability of this adsorbent was evaluated in view of the effects of solution pH, adsorbent dosage and contact time.

EXPERIMENTAL SECTION

Instrumentation

N_2 sorption analyses were performed on BELSORP-miniII at -196 °C. SBA-15 was degassed at 300 °C for 2 h but AEF-SBA-15 was degassed at 100 °C for 4 h. Specific surface area, total pore volume, and pore diameter of samples were obtained by Brunauer-Emmett-Teller (BET) method using BELSORP analysis software.

Scanning Electron Microscopy (SEM) images were taken by LEO 1455VP and morphology of pure SBA-15 and AEF-SBA-15 were investigated by these images.

ThermoGravimetric Analysis (TGA) measurements of pure SBA-15 and AEF-SBA-15 were performed on TA TGA Q50 in the temperature range from ambient to 800 °C. The ramp rate used was 20 °C/min.

The pH was controlled by Metrohm pH-meter model 713 and Varian UV/Vis spectrophotometer (Cary-100) was used for the detection of dye concentration in the solution.

Reagents and solutions

Tetraethyl orthosilicate (TEOS, Merck) as silica source, poly(ethylene glycol)-*block*-poly(propylene glycol)-*block*-poly(ethylene glycol) (P123, Aldrich) as surfactant, 3-[Bis(2-hydroxyethyl)amino]propyl-triethoxysilane solution (~%65 in ethanol, HPTES, Fluka) as amine compound, 2M hydrochloric acid prepared from concentrated hydrochloric acid (Merck), and ethanol (Merck) were used as received from suppliers.

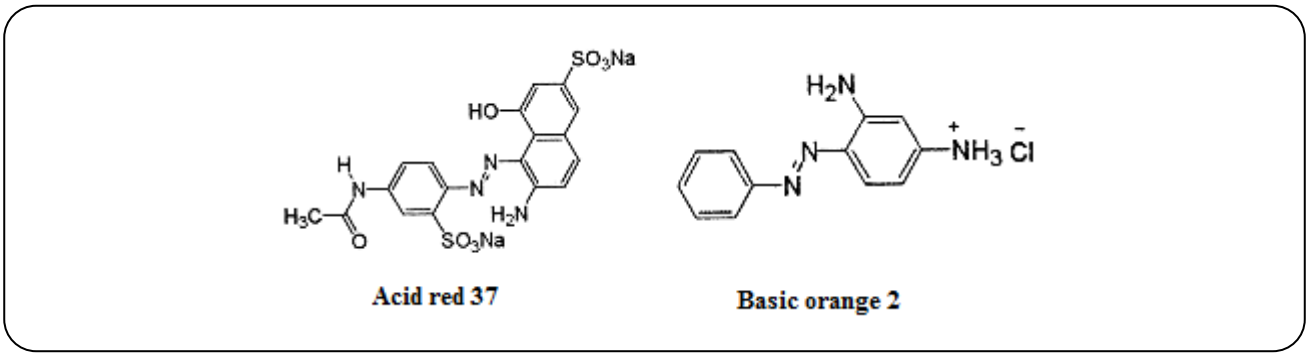

Fig. 1: Molecular structure of dyes (a): Acid red 37, (b): Basic Orange 2.

The commercial dyes Acid Red 37 (AR 37) an anionic dye with molecular weight 514.53 g/mol, Molecular Formula $C_{18}H_{16}N_4O_8S_2$ $2H_3N$ and Color Index Number: 17045, and Basic Orange 2 (BO 2) an cationic dye with molecular weight 248.71g/mol, Molecular Formula $C_{12}H_{13}ClN_4$ and Color Index Number: 11270 were purchased from Bayer (Germany). AR 37 and BO 2 dyes are dissociated anionic sulfonate and cationic ammonium in aqueous solution with the molecular structure, respectively. All the reagents were of analytical grade and used as received without further purification. Double Distilled Water (DDW) was used throughout the study. The stock solutions of dyes were prepared by dissolving dye powder in DDW. The stock solution was then diluted to prepare the desired concentration of dye solutions. All glassware were soaked in dilute nitric acid for 12 h and finally rinsed for three times with DDW prior to use.

Synthesis of Pure SBA-15

The preparation of SBA-15 was similar to the method reported by Zhao and coworkers [26]. 2 g of P123 was stirred with 15 mL of deionized water at 35°C until fully dissolved, followed by adding 30 g of 2 M HCl solution and drop wise addition of 4 g of TEOS. The mixture was allowed to stir at 35°C for 24 h before transferring into a Teflon bottle sealed in an autoclave, which was then heated to 100°C for 2 days in an oven. The solid was filtered off, washed three times with deionized water, and calcined at 600°C for 6h.

Synthesis of AEF-SBA-15

To prepare functionalized SBA-15 by post synthesis method, 1g calcined SBA-15 reacted with 0.065 g HPTES in 150 mL dry toluene under room temperature for 24 h. The resultant white solid was filtered off, washed with dry toluene, and dried at 80°C in an oven overnight. The schematic of the reaction was shown Fig. 2.

Dyes removal experiment

For each experimental run, sufficient amount of amino ethyl-functionalized nanoporous SBA-15 were added to 10 mL of 50 mg/L of each of dyes solutions with a predetermined concentration. The mixed solution was gently shacked at room temperature in sufficient time. At the end of the adsorption period, the supernatant was centrifuged for 2 min at 3750 rpm. The residual amounts of dyes in the solution were determined spectrophotometrically at 498 and 451 nm for Acid Red 37 (AR 37) and Basic Orange 2 (BO 2), respectively.

All the experiments were performed at room temperature. The effects of pH, contact time and dye concentration on adsorption were investigated. The adsorbed amounts (q_e) of dye were calculated by the following equation:

$$q_e = \frac{C_o - C_e}{m} \times V$$

Where C_o and C_e are the initial and equilibrium concentrations of dye in mg/L, m is the mass of adsorbent (g), and V is the volume of solution (L).

Equilibrium Study

The principle of adsorption isotherms is to find the relationship between the mass of the solute adsorbed per unit mass of adsorbent qe (mg/g) and the solute concentration in the solution at equilibrium Ce (mg/L). Equilibrium isotherms were analyzed by Freundlich and Langmuir isotherm models. The Freundlich isotherm

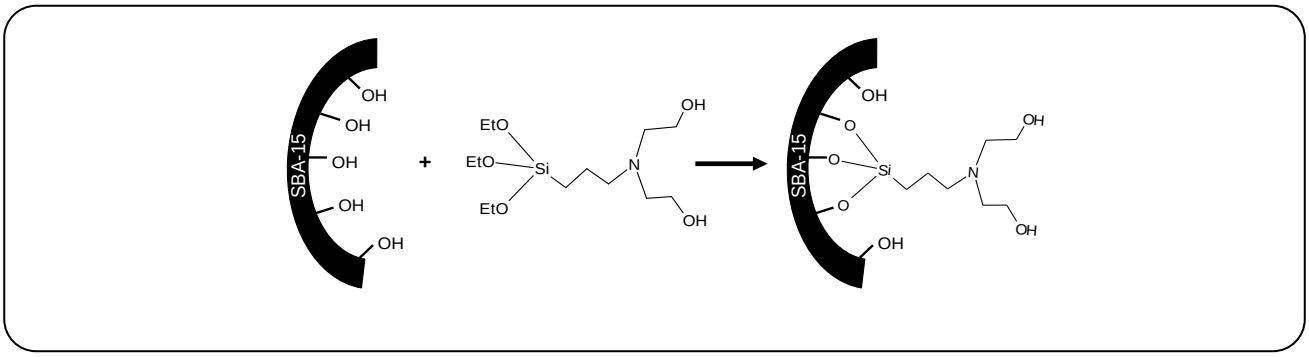

Fig. 2: Schematic illustration of modification of SBA-15 with 3-[Bis(2-hydroxyethyl)amino]propyl-triethoxysilane.

is derived by assuming a heterogeneous surface with a non-uniform distribution of heat of adsorption over the surface. Whereas, in the Langmuir theory, the basic assumption is that the sorption takes place at specific homogeneous sites within the adsorbent.

The linearized form of the Langmuir is [44]:

$$\frac{C_e}{q_e} = \frac{1}{bq_m} + \frac{C_e}{q_m}$$

Where q_m is the maximum adsorption capacity corresponding to complete monolayer coverage and b is the equilibrium constant (L/mg).

The Freundlich model can take the following linearized form [45]:

$$\log q_e = \log k_f + \frac{1}{n_f} \log C_e$$

Where K_f is is roughly an indicator of the adsorption capacity and $1/n_f$ is the adsorption intensity. The slope $1/n_f$ ranging between 0 and 1 is a measure of adsorption intensity or surface heterogeneity, becoming more heterogeneous as its value gets closer to zero [46].

For adsorption isotherm, the dye solutions with different concentrations in the range of 100-700 mg/L were agitated until the equilibrium was achieved. The dye adsorption capacities of the functionalized SBA-15 were measured individually at pH 5.0 with 10.0 mL varied AR37 and BO2 concentrations.

Standard addition calibration

Standard addition methods are particularly useful for analyzing complex samples in which the likelihood of matrix effects is substantial. A typical procedure involves preparing several solutions containing the same amount of unknown, but different amounts of the standard. In this study, four 50 mL volumetric flasks were each filled with 10 mL of the textile wastewater samples. Then the standard was added in differing amounts (0, 2, 4, and 6 mL of 1.5 mg/L). The flasks were then diluted to the mark and mixed well. The amounts of dyes in the solution were determined spectrophotometrically. After measuring the response for all of the solutions, the changes of absorption versus standard concentration were plotted. A simple Linear Least Squares analysis is made using the slope and intercept functions of Microsoft Excel. To find the original concentration of the unknown, the value of X at y=0 from y= mX+b was calculated.

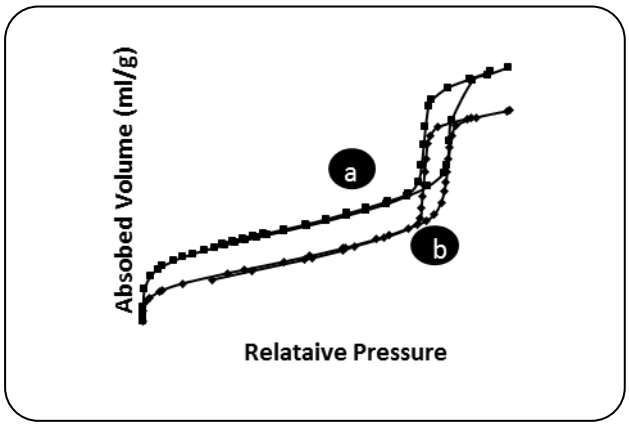

Fig. 3: Adsorption and desorption isotherms of a) SBA-15, and b) AEF-SBA-15 measured at - 196 °C.

RESULTS AND DISCUSSION

Characterization of amino ethyl-functionalized SBA-15

Fig. 3 shows the sorption isotherms before and after functionalization. As it seen in Fig. 3, the adsorption and desorption branches of pure and functionalized materials are parallel that can show the mesopores are still fully

Table 1: Specific surface area (S_{BET}), total pore volume (V_p), and pore diameter (D) for SBA-15 and AEF-SBA-15 obtained by BET method.

	$S_{BET}(m^2/g)$	$V_p(cm^3/g)$	D(nm)
Pure SBA-15	790	1.2862	7.06
AEF-SBA-15	520	0.9104	7.02

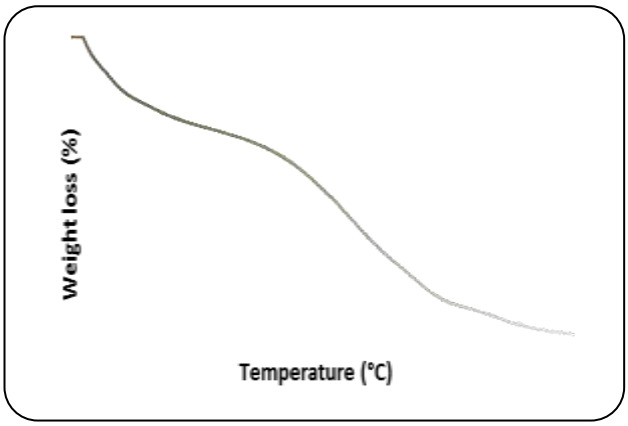

Fig. 4: TGA curve of AEF-SBA-15.

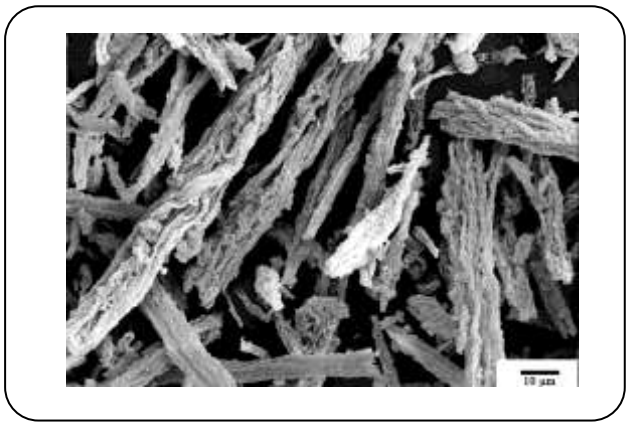

Fig. 5: SEM image of AEF-SBA-15.

accessible after functionalization. This reveals that no pore blocking takes place, which allows facile access for the chemical reagents or guest species.

The specific surface areas, total pore volumes, and mean pore diameters are shown in Table 1. In this research, no additional water was used, and then it can be concluded that functionalization was done on silanol capping approach and a slight decrease of pore diameter of AEF-SBA-15 rather than SBA-15 probably show this approach of functionalization.

The TGA curve of AEF-SBA-15 is shown in Fig. 4. There are four zones in the TGA curve: 1) weight loss up to 130 °C that refers to removal of physically adsorbed water, 2) slight weight loss between 130 and 250 °C that shows organic content of HPTES is thermally stable, 3) major weight loss (~%3.5) between 250 and 600 °C because of removal of organic content of HPTES, 4) slight weight loss between 600 and 800 °C, this is due to dehydroxylation of silicate networks [47] and/or elimination of residual ethoxy groups.

The SEM image of functionalized material is shown in Fig. 5. SEM image shows lengthy fiber-like morphology for the title material that arranged in a bundle of the diameter of ~10 μm and length of 30-60 μm. The same morphology was observed for SBA-15. It can be concluded that morphology of solid was saved without change.

Fig. 6 shows the low angle XRD patterns of SBA-15 and AEF-SBA-15. The samples have a single intensive reflection at 2θ angle around 1° as is the case for typical SBA-15 materials and the (100) reflection is generally attributed to the long-range periodic. For the SBA-15 material, two additional peaks corresponding to the higher ordering (110) and (200) reflections are also observed, which is associated with a two-dimensional hexagonal (p6mm) structure. However, the fact that peak (100) intensity decreases after immobilizations shows that the coupling agents causes the reduction of the peak intensity of diffraction. This is probably due to the difference in the scattering contrast of the pores and the walls, and to the erratic coating of organic groups on the nanochannels.

Effect of pH on the removal efficiency

The pH of the solution plays an important role in the chemistry of both dye molecules and the amino ethyl-functionalized nanoporous SBA-15 in aqueous solution. In addition, it has a significant effect on electrostatic charges that are imparted by ionized dye molecules between adsorbent and dyes. The effects of pH 2.0 to 8.0 on the adsorption of dyes are shown in Fig. 7. The pH was adjusted by HCl and NaOH and measured by digital pH meter. As shown in Fig. 6, the removal of the BO2 from aqueous solution was highly dependent

on the pH of the solution. The pH of the solution affected the surface charge of the functionalized nanoporous silica SBA-15 and the degree of ionization of the dyes.

For cationic dye BO 2, with an increase of pH, the adsorption capacity increased. This could be explained by the fact that, depending on pH, surface groups of adsorbent (N and OH) may change their charges. At low pH condition, most of the binding sites on ethyl-functionalized nanoporous SBA-15 are protonated and the surface of sorbents is surrounded by hydronium ions, thus inhibiting the binding of cationic BO2 dye molecules. With increasing pH of the dye solution, the surface groups will be deprotonated, resulting in an increase of negatively charged sites which favor the sorption of cationic dye (BO 2) due to electrostatic attraction. Therefore, the optimum pH for the removal of BO 2 is between 5- 8.

However, the opposite trend was observed for anionic dye (AR 37). Two sulfonates (–SO3−) groups of AR 37 dye are easily dissociated and have negative charges in the aquatic environment. At low pH, most of the surface groups of adsorbent (N and OH) will be protonated which is necessary for the attraction of anionic sulfonic groups. As the pH of the system decreases, the number of positively charged sites increases resulting in an increase of binding sites for anionic dye molecules. The deprotonation of surface groups in high pH range results in the electrostatic repulsion between the anionic dye and negatively charged sites. Therefore, the optimum pH for the removal of AR 37 is between 2- 7.5.

Effect of the amount of adsorbent on removal efficiency

The effect of the amount of amino ethyl-functionalized SBA-15 as adsorbent on the removal of acidic and basic dyes was determined at room temperature and at pH 5.0 by varying the adsorbent amount from 0.002 to 0.015 g in 10 mL solution of 50 mg/L of each dye. The results show (Fig. 8) that the removal efficiency of dyes initially was increased by increasing the amount of adsorbent due to the availability of higher adsorption sites. Then the percentage removal reaches almost a constant value. The 8 mg functionalized SBA-15 had a removal efficiency of 98% for AR37 and 45% for BO2. It indicates the high affinity between the AR 37 dye and the amino ethyl-functionalized SBA-15.

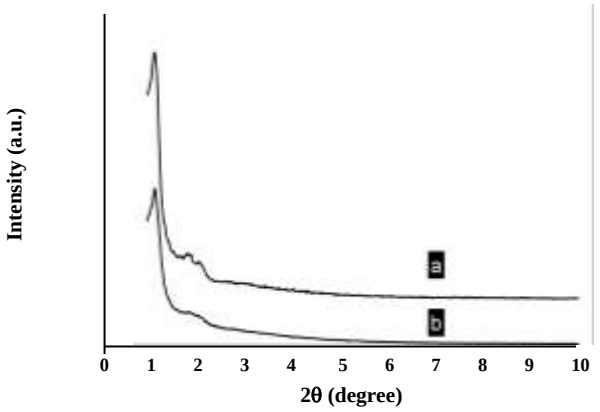

Fig. 6: XRD patterns of a) SBA-15 and b) AEF - SBA-15.

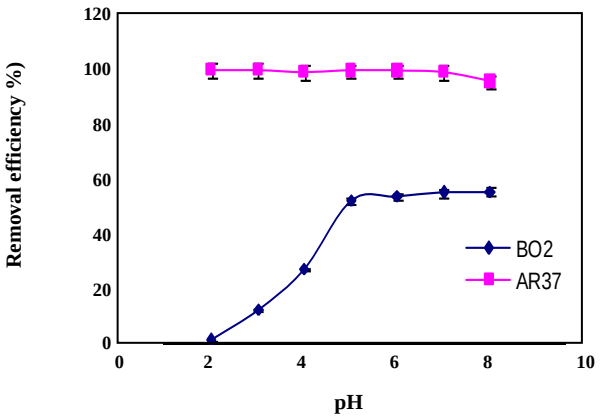

Fig. 7: The effect of pH on the adsorption of AR37 and BO2 on the AEF- SBA-15. Experiment conditions: sample volume: 10mL; concentration of analyte: 50 mg/L; adsorbent amount: 10 mg; contact time: 60 min.

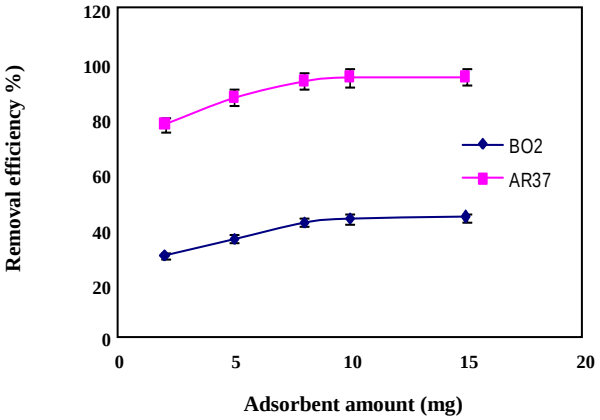

Fig. 8: The percentage of AR37 and BO2 dye removal using a different amount of AEF-SBA-15. Experiment conditions: sample volume: 10mL; concentration of analyte: 50 mg/L; pH of sample solution: 5; contact time: 60 min.

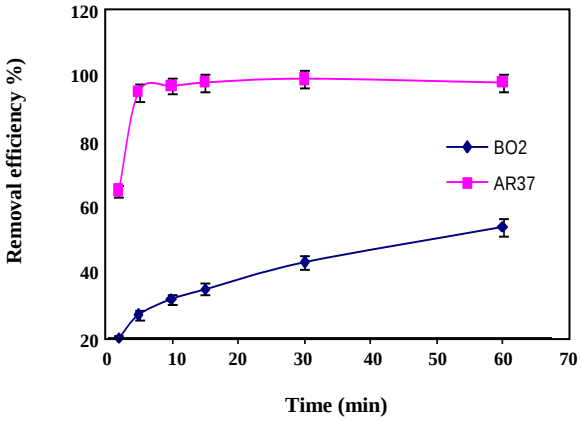

Fig. 9: The effect of contact time on the adsorption of AR37 and BO2 on AEF- SBA-15. Experiment conditions: sample volume: 10 mL; concentration of analyte: 50 mg/L; adsorbent amount: 8 mg; pH of sample solution: 5.

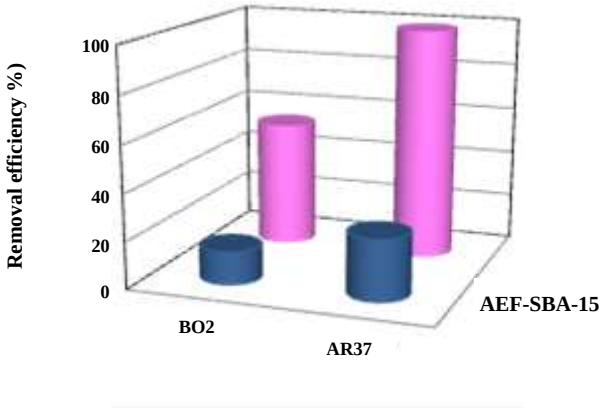

Fig. 10: The effect of the SBA-15 modification on the dyes removal efficiency. Experiment conditions: sample volume: 10 mL; concentration of analyte: 50 mg/L; adsorbent amount: 8 mg; pH of sample solution: 5; contact time: 5 min.

Effect of contact time

The kinetics of adsorption, which dictates the residence time of the adsorption is one of the most important tools to assess the adsorption efficiency. Therefore, the effect of contact time on a number of dyes adsorbed was investigated at the initial concentration of 50 mg/L of dyes at pH 5.0 at room temperature. The concentration of dyes was measured periodically in 2, 5, 10, 15, 30 and 60 minutes. Fig. 9 shows the effect of contact time on the removal yield of dyes by the amino ethyl-functionalized SBA-15. Almost, all of the AR 37 dye adsorbed after about 5 min, But BO 2 removal was up to above 45% after 60 min. It shows that the rate of BO 2 adsorption is very lower than AR 37 adsorption and confirms the high-affinity amino ethyl-functionalized SBA-15 for the AR 37 dyes. Also, t he whole adsorption process of dyes onto functionalized silica SBA-15 mainly included three phases: The initial rapid uptake phase, the slow uptake phase, and the equilibrium phase. At the initial stage due to a large number of vacant sites available, there existed highly concentration gradient between the dyes in solution and the dyes onto the adsorbent surface, thus led to increasing in dye sorption rate at initial stages. Afterward, as time proceed this concentration gradient and adsorption sites were reduced due to the accumulation of dye molecules in the vacant sites, the adsorption rate of the dye was smoothly increased and the finally reached equilibrium.

Effect of adsorbent modification

Effect of modification of SBA-15 on the dyes removal efficiency was investigated. In order to, eight mg of both unmodified SBA-15 and amino ethyl-functionalized nanoporous SBA-15 were added to 10 mL of 50 mg/L of each of dyes solutions. The mixed solution was gently shacked at room temperature for 5 min. Fig. 10 depict the percentage of removed dyes by modified and unmodified adsorbent. Remarkably, the removal efficiency of both dyes is very low in unmodified adsorbent and it is increased in modified adsorbent. The results have indicated that modification of adsorbent with a functional group of amino ethyl will remarkably increase the elimination of these two dyes.

Effect of initial dye concentration

Effect of initial concentration on the uptake of dyes was studied at different initial concentrations (100, 200, 300, 400, 500 and 700 mg/L). As expected, the overall trend was an increase of the adsorption capacity with increasing dye concentrations and this confirmed the strong chemical interaction between the dye molecules and adsorbent. As can be seen in Fig. 11, a number of dyes adsorbed increases as the concentration increases up to a saturation point. As long as there are available sites, adsorption will increase with increasing dye concentrations, but as soon as all of the sites are occupied, a further increase in concentrations of dyes does not increase the number of dyes on adsorbents.

Table 2: Isotherm parameters for adsorption of AR37 and BO2 dyes on AEF-SBA-15.

Dyes	Langmuir			Freundlich		
	q_m(mg/g)	b(L/mg)	R^2	K_f(mg g^{-1})	1/n	R^2
AR37	333.3	0.300	0.999	149.3	0.144	0.920
BO2	250.0	0.018	0.986	27.1	0.358	0.904

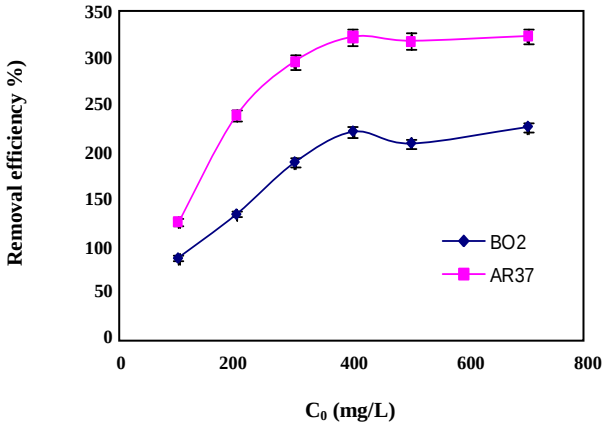

Fig. 11: The Langmuir adsorption isotherm of AR37 (a) and BO2 (b) on AEF-SBA-15. Experiment conditions: sample volume: 10 mL; adsorbent amount: 8 mg; pH of sample solution: 5; contact time: 5 min.

The unit adsorption for AR 37 increased from 124.2 to 321.9 mg/g with the increasing of AR 37 concentration from 100 to 700 mg/L and the adsorption amount for BO2 also increased from 86.2 to 225.0 mg/g as the BO2 concentration increased from 100 to 700 mg/L. It may be ascribed to the driving force of the concentration gradient increased as an increase in the initial dye concentration. The increase in initial dye concentration increases the number of collisions between dye and adsorbent [48].

Adsorption isotherms

In order to optimize the use of amino ethyl-functionalized nanoporous SBA-15, it is important to establish the most appropriate adsorption isotherm. The constants are determined by using linear regression analysis and are presented in Table 2. As seen from Table 2, the data fit well to the Langmuir isotherm model with correlation coefficients (R^2) in the range of 0.999 and 0.986 for AR33 and BO2 respectively. The Freundlich model is not suitable for describing the adsorption equilibrium of dyes by this adsorbent. Also, the maximum adsorption capacities of adsorbent are 333.3 mg/g and 250.0 mg/g for AR37 and BO2, respectively. Compared with BO2, the AR37 dye showed the higher adsorption capacity onto the amino ethyl-functionalized SBA-15. This means that the AEF-SBA-15 had a strong affinity for anionic dye AR37 in comparison with cationic BO2. In addition, a higher value of b for AR37 compared with BO2 confirmed higher affinity.

Desorption and reuse study

The reusability of adsorbent is of great importance as a cost effective process in water treatment. In order to regenerate and reuse the amino ethyl-functionalized SBA-15 after adsorbing dyes, 10 mL of 2.0 M sodium hydroxide solution and 10 mL 2.0 M hydrochloric Acid solution was selected as the regeneration agent for recovery of AR37 and BO2, respectively. Four cycles of adsorption-desorption studies were accordingly carried out. It is notable that the equilibrium of desorption was achieved rapidly within about 5 min. After the elution of the adsorbed dyes, the adsorbent was washed with DDW and dried under vacuum at 25°C and reused for dyes removal. The adsorption capacity of the sorbent after four cycles was reduced only 14% and 6% for AR37 and BO2, respectively, which was due to the incomplete desorption of dyes.

Removal of dyes from textile wastewater sample

The application of the AR37 and BO2 dyes removal from a real sample was examined by textile wastewater. To some sample solutions were added 40 mg/L of the each dye and to some of the solutions were added nothing. Because of matrix effect, the initial concentration and residual concentration of dyes in the samples (before and after removal with the recommended procedure) was determined by standard addition method. The results are given in Table 3. As shown, in high concentration of dyes, the proposed method could be applied successfully

Table 3: Removal of AR37 and BO2 dyes from textile wastewater samples.

Dyes	Added amount (mg/L)	Initial concentration (mg/L)	Final concentration (mg/L)	%Removal
AR37	----	0.04	0.01	75.0 (± 2.6) [a]
AR37	40	40.1	0.20	99.5 (± 1.9)
BO2	----	0.026	0.017	34.6 (± 2.4)
BO2	40	39.7	18.4	53.6 (± 2.0)

a) %RSD based on three replicate analysis

Table 4: Comparison of various adsorbents used for removal of AR37dye.

Adsorbent	Adsorption capacities (mg/g)	Ref.
Laccase-modified red mud	0.4412	49
Chitosan	128.21	50
Chitosan- ethylene glycol diglycidyl ether	59.52	50
Amino ethyl-functionalized SBA-15	333.3	This work

for the removing of AR37 dyes in wastewater samples with a very good efficiency of 99.5% and can remove more than half of BO2 amount in textile wastewater with a very complex matrix which is acceptable efficiency. Also, proposed adsorbent could remove AR37 and BO2 in very low concentration of dyes (75% for AR37 and 34% for BO2) whereas most of the adsorbents cannot be efficacious in these conditions.

Comparison of various adsorbents

The removal of AR37 by different adsorbents has been studied, and dye adsorption capacities were reported in literature [49-50]. Table 4 compares the adsorption capacity of the amino ethyl-functionalized SBA-15 with different adsorbents previously used for removal of AR37dye. The results are shown that the adsorption capacity of the amino ethyl-functionalized SBA-15 for the AR37 dye is much higher than that of other previously reported adsorbents, indicating that the amino ethyl-functionalized SBA-15 has great potential application in dye removal from aqueous solution.

CONCLUSIONS

This study has shown that the amino ethyl-functionalized nanoporous SBA-15 is an effective sorbent for the removal of Acid dye (AR 37) and Basic dye (BO2), from aqueous solution in single dye system. Modification of adsorbent with the functional group of amino ethyl will remarkably increase the elimination efficiency of these two dyes but amino ethyl-functionalized SBA-15 has higher affinity to AR37. The adsorption of dyes on functionalized SBA-15 was agreed well to the Langmuir adsorption model with maximum adsorption capacities of 333.3 and 250.0 mg/g for AR37 and BO2, respectively. The proposed method could be applied successfully for the removing of AR37 and BO2 dyes in textile wastewater samples with good and acceptable efficiency.

Acknowledgments

The author thanks the Islamic Azad University of Yadegar-e-Imam Khomeini (RAH) shahre-rey branch research council for support of this work.

Received :Nov. 24, 2015 ; Accepted : May 17, 2016

REFERENCES

[1] Ahmed M.J., Theydan S., Corrigendum to Equilibrium Isotherm and Kinetic Modeling of Methylene Blue Adsorption on Agricultural Wastes-Based Activated Carbons, *Fluid. Phase. Equilibr.*, **317**: 9-14 (2012).

[2] Qadri S., Ganoe, Haik A.Y., Removal and Recovery of Acridine Orange from Solutions by Use of Magnetic Nanoparticles, *J. Haz. Mater.*, **169**: 318-323 (2009).

[3] Qu S., Huang F., Yu S., Chen, G., Kong, J., Magnetic Removal of Dyes from Aqueous Solution Using Multi-Walled Carbon Nanotubes Filled with Fe_2O_3 Particles, *J. Haz. Mater.*, **160**: 643-647. (2008).

[4] Chen S., Zhang J., Zhang C., Yue Q., Li Y., Li C., Equilibrium and Kinetic Studies of Methyl Orange and Methyl Violet Adsorption on Activated Carbon Derived from Phragmites Australis, *Desalination*, **252**(1): 149-156 (2010).

[5] Pugazhenthiran N., Ramkumar S., Kumar P.S., Anandan S., In-situ Preparation of Heteropolytungstic Acid on TiMCM-41 Nanoporous Framework for Photocatalytic Degradation of Textile Dye Methyl Orange, *Microp. Mesop. Mater.*, **131**(1-3): 170-176 (2010).

[6] Crini G., Non-conventional Low-Cost Adsorbents for Dye Removal: a Review, *Bioresour Technol.*, **97**(9): 1061-1085 (2006).

[7] Oei B.C., Ibrahim S., Wang S., Ang H.M., Surfactant Modified Barley Straw for Removal of Acid and Reactive Dyes from Aqueous Solution, *Bioresour Technol.*, **100**(8): 4292-4295 (2009).

[8] Jalil A.A., Triwahyono S., Adama S.H., Rahima N.D., Aziz M.A.A., Hairomc N.H.H., Razali N.A.M., Abidin M. A.Z., Khairul M., Mohamadiah A., Adsorption of Methyl Orange from Aqueous Solution Onto Calcined Lapindo Volcanic Mud, *J. Hazard. Mater.*, **181**: 755-762 (2010).

[9] Cheung W.H., Szeto Y.S., McKay G., Enhancing the Adsorption Capacities of Acid Dyes by Chitosan Nano Particles, *Bioresour Technol.*, **100**(3): 1143-1148 (2009).

[10] Samarghandi M.R., Zarrabi M., Noori S., Mohammad Panahi R., Foroghi M., Removal of Acid Red 14 by Pumice Stone as a Low-Cost Adsorbent: Kinetic and Equilibrium Study, *Iran. J. Chem. Chem. Eng. (IJCCE)*, **31**(3): 19-27 (2012).

[11] Ferrero F., Adsorption of Methylene Blue on Magnesium Silicate: Kinetics, Equilibria, and Comparison with Other Adsorbents, *J. Environ. Sci.*, **22**(3): 467-473 (2010).

[12] Li, L., Liu, S., Zhu, T., Application of Activated Carbon Derived from Scrap Tires for Adsorption of Rhodamine B, *J. Environ. Sci.*, **22**(8): 1273-1280 (2010).

[13] Mittal, A., Gupta, V.K., Malviya, A., Mittal, J., Process Development for the Batch and Bulk Removal and Recovery of a Hazardous, Water-Soluble Azo Dye (Metanil Yellow) by Adsorption Over Waste Materials (Bottom Ash and De-Oiled Soya), *J. Hazard. Mater.* 1**51**: 821-832 (2008).

[14] Naseri A., Barati R., Rasoulzadeh F., Bahram M., Studies on Adsorption of Some Organic Dyes from Aqueous Solution onto Graphene Nanosheets, *Iran. J. Chem. Chem. Eng. (IJCCE)*, **34**(2): 51-60 (2015).

[15] Pourbabaee A.A., Malekzadeh F., Sarbolouk M.N., Mohajeri A., Decolorization of Methyl Orange (As a Model Azo Dye) by the Newly Discovered Bacillus Sp, *Iran. J. Chem. Chem. Eng. (IJCCE)*, **24**(3): 41-45 (2005).

[16] Chang S.H., Wang K.S., Li H.C., We M.Y., Chou J.D, Enhancement of Rhodamine B Removal by Low-Cost Fly Ash Sorption with Fenton Pre-Oxidation, *J. Hazard. Mater.*, **172**(2-3): 1131-1136 (2009).

[17] Zhao K., Zhao G., Li P., Gao J., Lv B., Li, D., A Novel Method for Photodegradation of High-Chroma Dye Wastewater via Electrochemical Pre-Oxidation, *Chemosphere*, **80**(4): 410-415 (2010).

[18] Alizadeh M., Ghahramani E., Zarrabi M., Hashemi S., Efficient De-Colorization of Methylene Blue by Electro-coagulation Method: Comparison of Iron and Aluminum Electrode, *Iran. J. Chem. Chem. Eng. (IJCCE)*, **34**(1): 39-47 (2015).

[19] Rajeev J., Megha M., Shalini S., Alok, M., Removal of the Hazardous Dye Rhodamine B Through Photocatalytic and Adsorption Treatments, *J. Environ. Manage*., **85**(4): 956-964 (2007) DOI: 10.1016/j.jenvman.2006.11.002.

[20] Wang S., Li H., Xu L., Application of Zeolite MCM-22 for Basic Dye Removal from Wastewater, *J. Colloid Interface Sci.*, **295**(1): 71–78 (2006).

[21] Yuan X., Zhuo S.P., Xing W., Cui H.Y., Dai X.D., Liu X.M., Yan Z.F., Aqueous Dye Adsorption on Ordered Mesoporous Carbons, *J. Colloid Interface Sci.*, **310**(1): 83–89 (2007).

[22] Huang C.H., Chang K.P., Ou H.D., Chiang Y.C., Wang C.F., Adsorption of Cationic Dyes Onto Mesoporous Silica, *Microp. Mesop. Mater.*, **141**(1-3): 102–109 (2011).

[23] Beck J.S., Vartuli J.C., Roth W.J., Kresge C.T., Leonowicz M.E., Schmitt K.D., Chu C.T.W., Olson D.H., Sheppard E.W., McCullen S.B., Higgins J.B., Schlenker J.L., A New Family of Mesoporous Molecular Sieves Prepared with Liquid Crystal Templates, *J. Am. Chem. Soc.*, **114**(27): 10834-10843 (1992).

[24] Reinert P., Garcia B., Morin C., Badiei A., Perriat P., Tillement O., Bonneviot L., Cationic Templating with Organic Counterion for Superstable Mesoporous Silica, *Stud. Surf. Sci. Catal.*, **146**: 133 (2003).

[25] Bonneviot L., Morin M., Badiei A., Mesostructured Metal or Non-Metal Oxides and Method for Making Same, *Patent WO 2001/055031 A1*, (2001).

[26] Zhao D., Huo Q., Feng J., Chmelka B.F., Stucky G.D., Nonionic Triblock and Star Diblock Copolymer and Oligomeric Surfactant Syntheses of Highly Ordered, Hydrothermally Stable, Mesoporous Silica Structures, *J. Am. Chem. Soc.* **120**(24): 6024-6036 (1998).

[27] Goscianska J., Marciniak M., Pietrzak R., Ordered Mesoporous Carbons Modified with Cerium as Effective Adsorbents for Azo Dyes Removal, *Separation, and Purification Technology*, **154**: 236-245 (2015).

[28] Goscianska J., Ptaszkowska M., Pietrzak R., Equilibrium and Kinetic Studies of Chromotrope 2R Adsorption Onto Ordered Mesoporous Carbons Modified with Lanthanum, *Chemical Engineering Journal*, **270**: 140–149 (2015).

[29] Goscianska J., Pietrzak R., Removal of Tartrazine from Aqueous Solution by Carbon Nanotubes Decorated with Silver Nanoparticles, *Catalysis Today*, **249**: 259–264 (2015).

[30] Trong On D., Desplantier-Giscard D., Danumah C., Kaliaguine S., Perspectives in Catalytic Applications of Mesostructured Materials, *Appl. Catal. A: Gen.*, **359(2)**: 299-357 (2001).

[31] Ganjali M.R., Daftari A., Hajiagha Babaei L., Badiei A., Saberyan K., Mohammadi Ziarani G., Moghimi A., Pico Level Monitoring of Silver with Modified Hexagonal Mesoporous Compound (MCM-41) and Inductively Coupled Plasma Atomic Emission Spectrometry, *Water, Air, and Soil Pollution*, **173**(1): 71-80 (2006).

[32] Gangali M.R., Hajiagha Babaei L., Badiei A., Mohammadi Ziarani G., Tarlani A., Novel Method for the Fast Preconcentration and Monitoring of a ppt Level of Lead and Copper with a Modified Hexagonal Mesoporous Silica Compound and Inductively Coupled Plasma Atomic Emission Spectrometry, *Anal. Sci.*, **20**: 725-729 (2004).

[33] Ganjali M.R., Hajiagha Babaei L., Badiei A., Saberian K., Behbahani S., Mohammadi Ziarani G., Salavati- Niasari M., A Novel Method for Fast Enrichment and Monitoring of Hexavalent and Trivalent Chromium at the ppt Level with Lodified Silica MCM-41 and Its Determination by Inductively Coupled Plasma Optical Emission Spectrometry, *Quim. Nova*, **29**(3): 440-443 (2006).

[34] Zhu S., Zhou Z., Zhang D., Jin C., Li Z., Design and Synthesis of Delivery System Based on SBA-15 with Magnetic Particles Formed in Situ and Thermo-Sensitive PNIPA as Controlled Switch, *Microp. Mesop. Mater.*, **106**(1-3): 56–61 (2007).

[35] Badiei A., Norouzi P., Tousi F., Study of Electrochemical Behavior and Adsorption Mechanism of [Co(en)2Cl2] + on Mesoporous Modified Carbon Paste Electrode, *Europ. J. Scien. Res.*, **12**(1): 39-45. (2005).

[36] Ho K.Y., Mckay G., Yeung K.L., Selective Adsorbents from Ordered Mesoporous Silica, *Langmuir*, **19**(7): 3019-3024 (2003).

[37] Anbia M., Asl Hariri S., Ashrafizadeh S.N., Adsorptive Removal of Anionic Dyes by Modified Nanoporous Silica SBA-3, *Appl. Surface Sci.*, **256**(10): 3228–3233 (2010).

[38] Anbia M., Salehi S., Removal of Acid Dyes from Aqueous Media by Adsorption Onto Amino-Functionalized Nanoporous Silica SBA-3, *Dyes and Pigments*, **94**(1): 1-9 (2012).

[39] Goscianska J., Olejnik A., Pietrzak R., Adsorption of L-phenylalanine Onto Mesoporous Silica, *Materials Chemistry and Physics*, **142**: 586–593 (2013).

[40] Zhao D., Feng J., Huo Q., Melosh N., Fredrckson G.H., Chmelka B.F., Stucky G.D., Triblock Copolymer Syntheses of Mesoporous Ssilica with Periodic 50 to 300 Angstrom Pores, *Science*, **279**(5350): 548-552 (1998).

[41] Da'n a E., Sayari A., Adsorption of Copper on Amine-Functionalized SBA-15 Prepared by Co-Condensation: Equilibrium Properties, *Chem. Eng. J.*, **166**(1): 445–453 (2011).

[42] Da'na E., De Silva N., Sayari A., Adsorption of Copper on Amine-Functionalized SBA-15 Prepared by Co-Condensation: Kinetics Properties, *Chem. Eng. J.*, **166**(1): 454–459 (2011).

[43] Badiei A., Bonneviot L., Crowther N., Mohammadi Ziarani G., Surface Tailoring Control in Micelle Templated Silica, *J. Organomet. Chem.*, **691**: 5923-5931 (2006).

[44] Langmuir I., Adsorption of Gases on Plain Surface of Mica Platinum, *J. Am. Chem. Soc.*, **40**, 136-403 (1918).

[45] Freundlich H.M.F., Over the Adsorption in Solution, *J. Phys. Chem.*, **57**: 385-470 (1906).

[46] Haghseresht F., Lu G., Adsorption Characteristic of Phenolic Compounds Onto Coal Reject-Derived Adsorbents, *Energy Fuels*, **12**(6): 1100-1107 (1998).

[47] Zhao X.S., Lu G.Q., Whittaker A.K., Millar G.J., Zhu H.Y., Comprehensive Study of Surface Chemistry of MCM-41 Using 29Si CP/MAS NMR, FTIR, Pyridine-TPD, and TGA, *J. Phys. Chem. B*, **101**(33): 6525-6531 (1997).

[48] Mohammadi N., Khani H., Gupta V.K., Adsorption Process of Methyl Orange Dye Onto Mesoporous Carbon Material-Kinetic and Thermodynamic Studies, *J. Colloid. Interf. Sci.*, **362**(2): 457–462 (2011).

[49] Nadaroglu H., Kalkan E., Celebi N., Azo Dye Removal from Aqueous Solutions Using Laccase-modified Red Mud: Adsorption Kinetics and Isotherm Studies, *Annual Research & Review in Biology*, **4(17)**: 2730-2754 (2014).

[50] Azlan K., Wan Saime W.N., Lai Ken L., Chitosan and Chemically Modified Chitosan Beads for Acid Dyes Sorption, *J. Environ. Sci. (China)*, **21(3)**: 296-302 (2009).